CHARACTERIZATION OF NONLINEAR LOADS
IN POWER DISTRIBUTION GRID

Miona Andrejević Stošović[1], Marko Dimitrijević[1], Slobodan Bojanić[2],
Octavio Nieto-Taladriz[2], Vančo Litovski[1]

[1]University of Niš, Faculty of Electronic Engineering, Niš, Serbia
[2]Escuela Técnica Superior de Ingenieros de Telecomunicación,
Universidad Politecnica de Madrid, Madrid, Spain

Abstract. *Electronic devices are complex circuits, consisting of analog, switching, and digital subsystems that require direct current (DC) for polarization. Since they are connected to the mains delivering alternating current (AC), however, AC-to-DC converters are to be introduced between the mains and the electronics to be fed. A converter is an electric circuit containing several subsystems, the most important being the switch-mode power supply, drawing power from the mains in pulses hence it is highly nonlinear. That happens, in reduced amplitude, even when the electronics to be fed is switched off. The process of AC-to-DC conversion is not restricted to feeding electronic equipment only. It is more and more frequently encountered in modern smart-grid facilities giving rise to the importance of the studies referred hereafter. The converter can be studied (theoretically or by measurements) as two-port network with reactive and nonlinear port-impedances. Characterization is performed after determining the port electrical quantities which are voltages and currents. Based on these data power and power quality parameters – power factor and total harmonic distortion- may be extracted. When nonlinear loads are present, one should introduce new ways of thinking into the considerations due to the existence of harmonics and related power components. In that way the power factor can be generalized to total or true power factor where the apparent power, involved in its calculations, includes all harmonic components. After introducing a wide range of definitions used in contemporary literature, here we describe our measurement set-up both as hardware and a software solution. The results reported unequivocally confirm the importance of the subject of characterization of small nonlinear loads to the grid having in mind their number which is rising without saturation seen in the near and even far future.*

Key words: *smart grid, nonlinear loads, load characterization, power factor, harmonic distortions*

1. INTRODUCTION

With the advent of modern diversified sources of electrical energy, the issue of power quality becomes both more ambiguous and more complicated. We will address here first the new aspects that are coming in fore thanks to the new ways of producing electrical energy, which are becoming more and more popular, and thanks to the emergence of a new paradigm known as smart-grid which involves mutual interaction of power electrical systems and electronic systems for its proper functionality [1].

Nowadays we are witnessing changes in the demand and energy use which in fact means "new" load characteristics, and trends changing the nature of the aggregate utility consumption. All of that is mostly due to the electronic devices that became ubiquitous. It is presumed that the overall household consumption for electronic appliances will rise with a rate of 6% per year so reaching 29% of the total household consumption in the year 2030. In the same time the household consumption is expected to reach 40% of the overall electricity demand. The immense rise of the office consumption due to the enormous number of computers in use is also to be added. That stands for educational, administrative, health, transport, and other public services, too. One may get the picture if one multiplies the average consumption of a desk-top (about 120 W) with the average number of hours per day when the computers is on (about 7), and the number of computers (billion(s)?).

Electronic loads are strongly related to the power quality thanks to the implementation of AC/DC converters that in general draw current from the grid in bursts. The current voltage relationship of these loads, looking from the grid side, is nonlinear, hence nonlinear loads.

In fact, while keeping the voltage waveform almost sinusoidal, they impregnate pulses into the current so chopping it into seemingly arbitrary waveform and, consequently, producing harmonic distortions. Having all this in mind the means for characterization of the load from the nonlinearity point of view becomes one of the inevitable tools of quality evaluation of smart grid.

The problem is further complicated when different power generation technologies and resources are combined leading. New subsystem in the power production, transport, and consumption emerge named micro-grids and the overall system is supposed to become a smart-grid. For example, due to the rise of the number of different kind of electricity sources even the frequency of the grid voltage may be considered as "unknown" asking for algorithms and software to be implemented in real time to extract the frequency value [2] and, based on that, to compute the amplitudes of the harmonics [3, 4, 5].

Due to the nonlinearities, measurement of power factor and distortion, however, usually requires dedicated equipment. For example, use of a classical ammeter will return incorrect results when attempting to measure the AC current drawn by a non-linear load and then calculate the power factor. A true RMS multi-meter must be used to measure the actual RMS currents and voltages and apparent power. To measure the real power or reactive power, a wattmeter designed to properly work with non-sinusoidal currents must be also used.

Contemporary methods and algorithms for spectrum analysis are presented in this paper. The basic definitions of parameters describing nonlinear loads are introduced. Alternative definitions for reactive power and their calculation methods are elaborated, also.

In our previous research we were first developing a tool for efficient measurements that would allow for proper and complete characterization of the nonlinear loads [6, 7]. Namely we found that the tools for characterization of modern loads available on the market, most frequently, lack at least one of the following properties: low price, ability of implementation of complex data processing algorithms (versatility), ability to store and

statistically analyze the measured data, and ability to communicate with its environment no matter how distant it is. All these were achieved by the system reported in [6, 7] and the measurement results demonstrated here were obtained by these tools.

Next, we implemented these tools for characterization of small loads. The results obtained, as reported in [8] and [9] for example, were, in some cases, surprisingly different from what expected. That stands for the power components which are not the active power and for the abundance of harmonics. In [10] and [11] we demonstrated that based on the main's current, by proper data processing, despite the complex signal transformation between the mains and the components of a computer via the power supply chain, one may deduce the activities within the computer. Even more, one may recognize a software running within the computer. Such information is distributed via the grid.

Here we will for the first time summarize the theoretical background of all computations necessary to be performed for complete characterization of small loads. Then, we will demonstrate our new results in the implementation of the theory and the measurement tools on a set of nonlinear loads.

The definitions used in modern characterization of the main's current, voltage, and power which are implemented by our system will be listed in the second section so enabling the main attention to be devoted to the set of measured results and their analysis, which will be given next.

The paper will be organized as follows. First a short description of the measurement experiment will be given. To preserve conciseness, for this purpose, we will mainly refer to our previous work.

2. PARAMETER DEFINITIONS

Although power quality is a relatively ambiguous concept, limited mostly to conversations among utility engineers and physicists, as electronic appliances take over the home, it may become a residential issue as well.

2.1. Linear loads with sinusoidal stimuli

A sinusoidal voltage source

$$v(t) = \sqrt{2}V_{\text{RMS}}\sin(\omega t) \tag{1}$$

supplying a linear load, will produce a sinusoidal current of

$$i(t) = \sqrt{2}I_{\text{RMS}}\sin(\omega t - \varphi) \tag{2}$$

where V_{RMS} is the RMS value of the voltage, I_{RMS} is the RMS value of the current, ω is the angular frequency, φ is the phase angle and t is the time. The instantaneous power is

$$p(t) = v(t) \cdot i(t) \tag{3}$$

and it can be represented as

$$p(t) = 2V_{\text{RMS}}I_{\text{RMS}}\sin\omega t \cdot \sin(\omega t - \varphi) = p_p + p_q. \tag{4}$$

Using trigonometric transformations, we can write:

$$p_p = V_{\text{RMS}} \cdot I_{\text{RMS}} \cdot \cos\varphi \cdot (1 - \cos(2\omega t)) = P \cdot (1 - \cos(2\omega t)) \tag{5}$$

and

$$p_q = -V_{RMS} \cdot I_{RMS} \cdot \sin\varphi \cdot \sin(2\omega t) = -Q \cdot \sin(2\omega t) \tag{6}$$

where

$$
\begin{aligned}
P &= V_{RMS} \cdot I_{RMS} \cdot \cos\varphi, \\
Q &= V_{RMS} \cdot I_{RMS} \cdot \sin\varphi
\end{aligned}
\tag{7}
$$

represent real (P) and reactive (Q) power.

It can be easily shown that the real power presents the average of the instantaneous power over a cycle:

$$P = \frac{1}{T} \int_{t_0}^{t_0+T} v(t) \cdot i(t) \cdot dt \tag{8}$$

where t_0 is arbitrary time (constant) after equilibrium, and T is the period (20ms in European and 1/60s in American system, respectively).

The reactive power Q is the amplitude of the oscillating instantaneous power p_q. The apparent power is the product of the root mean square value of current times the root mean square value of voltage:

$$S = V_{RMS} \cdot I_{RMS} \tag{9}$$

or:

$$S = \sqrt{P^2 + Q^2}. \tag{10}$$

Power factor is simply defined as the ratio of real power to apparent power [12, 3]:

$$TPF = P/S. \tag{11}$$

For pure sinusoidal case, using (7), (10) and (11) we can calculate:

$$TPF = \cos\varphi. \tag{12}$$

2.2. Nonlinear loads

When there is a nonlinear load in the system, it operates in non-sinusoidal condition and use of well known parameters such as power factor, defined as cosine of phase difference, does not describe system properly. In that case, traditional power system quantities such as effective value, power (active, reactive, apparent), and power factor need to be numerically calculated from sampled voltage and current sequences by performing DFT, FFT or Goertzel algorithm [3].

The RMS value of some periodic physical entity X (voltage or current) is calculated according to the well-known formula [13, 14]:

$$X_{RMS} = \sqrt{\frac{1}{T} \int_{t_0}^{t_0+T} (x(t))^2 dt} \tag{13}$$

where $x(t)$ represents time evolution, T is the period and t_0 is arbitrary time. For any periodic physical entity $x(t)$, we can give Fourier representation:

$$x(t) = a_0 + \sum_{k=1}^{+\infty} (a_k \cdot \cos(k\omega t) + b_k \cdot \sin(k\omega t)) \tag{14}$$

or

$$x(t) = c_0 + \sum_{k=1}^{+\infty} c_k \cdot \cos(k\omega t + \psi_k) \tag{15}$$

where $c_0 = a_0$ represents DC component, $c_k = \sqrt{a_k^2 + b_k^2}$ magnitude of kth harmonic, $\psi_k = \arctan(b_k/a_k)$ phase of kth harmonic and $\omega = 2\pi/T$, angular frequency.

Fourier coefficients a_k, b_k are:

$$a_0 = \frac{1}{T} \int_{-T/2}^{+T/2} x(t) dt, \quad a_k = \frac{2}{T} \int_{-T/2}^{+T/2} x(t) \cdot \cos\left(\frac{2k\pi t}{T}\right) dt \tag{16}$$

and

$$b_k = \frac{2}{T} \int_{-T/2}^{+T/2} x(t) \cdot \sin\left(\frac{2k\pi t}{T}\right) dt. \tag{17}$$

The RMS value of kth harmonic is

$$X_{k,\text{RMS}} = c_k / \sqrt{2}. \tag{18}$$

We can calculate total RMS value

$$X_{\text{RMS}} = \sqrt{\sum_{k=1}^{M} X_{k,\text{RMS}}^2} = \sqrt{X_{1,\text{RMS}}^2 + X_{\text{H,RMS}}^2} \tag{19}$$

where M is the highest order harmonic taken into calculation. Index "1" denotes first or fundamental harmonic, and index "H" denotes contributions of higher harmonics.

Equations (13) – (19) need to be rewritten for voltage and current. Practically, we operate with sampled values and integrals (16) and (17) are transformed into finite sums.

For a single-phase system where k is the harmonic number, φ_k phase difference between voltage and current of kth harmonic and M is the highest harmonic, the total active power is given by:

$$P = \sum_{k=1}^{M} I_{k,\text{RMS}} \cdot V_{k,\text{RMS}} \cdot \cos\varphi_k = P_1 + P_{\text{H}}. \tag{20}$$

The first addend in the sum (20), denoted with P_1, is fundamental active power. The rest of the sum, denoted with P_{H}, is harmonic active power [13].

In the literature, there exists a number of definitions of reactive power for non-sinusoidal conditions that serve to characterize nonlinear loads and measure the degree of loads' non-linearity [14]. As more general term, non-active power N, was introduced. Each definition has some advantages over others. But, although there is tendency to generalize, there is no generally accepted definition.

The most common definition of reactive power is Budeanu's definition [15], given by following expression for single phase circuit:

$$Q_{\text{B}} = \sum_{k=1}^{+\infty} I_{k,\text{RMS}} \cdot V_{k,\text{RMS}} \cdot \sin\varphi_k. \tag{21}$$

Budeanu proposed that apparent power consists of two orthogonal components, active power (20) and non-active power, which is divided into reactive power (21) and distortion power:

$$D = \sqrt{U^2 - P^2 - Q_{\mathrm{B}}^2}. \tag{22}$$

It should be noted that the actual contribution of harmonic frequencies to active and reactive power is small (usually less than 3% of the total active or reactive power). The major contribution of higher harmonics to the power comes as distortion power.

The apparent power, for non-sinusoidal conditions conventionally denoted as U, can be written:

$$U^2 = \underbrace{I^2_{1,\mathrm{RMS}} \cdot V^2_{1,\mathrm{RMS}}}_{S_1^2} + \underbrace{I^2_{1,\mathrm{RMS}} \cdot V^2_{H,\mathrm{RMS}}}_{D_V^2} + \\ + \underbrace{V^2_{1,\mathrm{RMS}} \cdot I^2_{H,\mathrm{RMS}}}_{D_I^2} + \underbrace{V^2_{H,\mathrm{RMS}} \cdot I^2_{H,\mathrm{RMS}}}_{S_{\mathrm{H}}^2} \tag{23}$$

where S_1 represents fundamental apparent power, D_{V} voltage distortion power, D_{I} current distortion power and S_{H} harmonic apparent power. S_1 and S_{H} are

$$S_1 = \sqrt{P_1^2 + Q_1^2}, \; S_{\mathrm{H}} = \sqrt{P_{\mathrm{H}}^2 + Q_{\mathrm{H}}^2 + D_{\mathrm{H}}^2} \tag{24}$$

where D_{H} represents harmonic distortion power. The total apparent power, denoted with U, is

$$U = \sqrt{P^2 + Q^2 + D^2} = I_{\mathrm{RMS}} \cdot V_{\mathrm{RMS}}. \tag{25}$$

We can also define non-active power N, defined with equation

$$N = \sqrt{Q^2 + D^2} \tag{26}$$

and phasor power S, defined in the same way as apparent power for sinusoidal conditions (10). It is obvious that for sinusoidal conditions, apparent power and phasor power are equal, and (25) reduces to (10).

The total harmonic distortions, THD, are calculated from the following formula [12, 13]:

$$THD_I = \frac{I_{\mathrm{H, RMS}}}{I_{1,\mathrm{RMS}}} = \frac{1}{I_{1,\mathrm{RMS}}} \sqrt{\sum_{j=2}^{M} I^2_{j,\mathrm{RMS}}} = \sqrt{\frac{I_{\mathrm{RMS}}^2 - I^2_{1,\mathrm{RMS}}}{I^2_{1,\mathrm{RMS}}}} \tag{27}$$

and

$$THD_V = \frac{V_{\mathrm{H},RMS}}{V_{1,RMS}} = \frac{1}{V_{1,RMS}} \sqrt{\sum_{k=2}^{M} V^2_{k,\mathrm{RMS}}} = \sqrt{\frac{V_{\mathrm{RMS}}^2 - V^2_{1,\mathrm{RMS}}}{V^2_{1,\mathrm{RMS}}}} \tag{28}$$

where I_j, V_k j, k=1, 2, …, M stands for the harmonic of the current or voltage. It can be shown that:

$$D_I = V_{1,\mathrm{RMS}} \cdot I_{\mathrm{H,RMS}} = S_1 \cdot THD_I \\ D_V = V_{\mathrm{H,RMS}} \cdot I_{1,\mathrm{RMS}} = S_1 \cdot THD_V \\ S_H = S_1 \cdot THD_I \cdot THD_V. \tag{29}$$

Fundamental power factor or displacement power factor is given by the following formula:

$$PF_1 = \frac{P_1}{S_1} = \cos\varphi_1. \tag{30}$$

Total power factor TPF [12, 13], defined by equation (12), taking into calculation (11) and (23), is

$$TPF = \frac{P}{U} = \frac{P_1 + P_H}{\sqrt{S_1^2 + D_I^2 + D_V^2 + U_H^2}} \tag{31}$$

and substituting (29) and (30):

$$TPF = \frac{\left(1 + \dfrac{P_H}{P_1}\right)\cos\varphi_1}{\sqrt{1 + THD_I^2 + THD_V^2 + \left(THD_I \cdot THD_V\right)^2}}. \tag{32}$$

Total power factor can be represented as product of distortion power factor DPF and displacement power factor PF1, i.e. $\cos\varphi_1$:

$$TPF = DPF \cdot \cos\varphi_1 \tag{33}$$

Therefore, distortion power factor is [12, 13]

$$DPF = \frac{1 + \dfrac{P_H}{P_1}}{\sqrt{1 + THD_I^2 + THD_V^2 + \left(THD_I \cdot THD_V\right)^2}}. \tag{34}$$

In real circuits, $P_H \ll P_1$ and voltage is almost sinusoidal ($THD_V < 5\%$), leading to simpler equation for TPF [12, 13]:

$$TPF = \frac{\cos\varphi_1}{\sqrt{1 + THD_I^2}}. \tag{35}$$

2.3. Other definitions of reactive power

Budeanu's definition

The most common definition of reactive power is Budeanu's definition [16], given by following expression for single phase circuit, as mentioned earlier in the text:

$$Q_B = \sum_{k=1}^{+\infty} I_{k,\text{RMS}} \cdot V_{k,\text{RMS}} \cdot \sin\varphi_k \tag{36}$$

Budeanu proposed that apparent power consists of two orthogonal components, active power and non-active power, which is divided into reactive power (36) and distortion power:

$$D_B = \sqrt{U^2 - P^2 - Q_B^2}. \tag{37}$$

IEEE Std 1459-2010 proposes reactive power to be calculated as:

$$Q_{\text{IEEE}} = \sqrt{\sum_{k=1}^{+\infty} I_{k,\text{RMS}}^2 \cdot V_{k,\text{RMS}}^2 \cdot \sin^2\varphi_k} \tag{38}$$

Equation (38)eliminates the situation where the value of the total reactive power Q is less than the value of the fundamental component.

Kimbark's definition

Similar to Budeanu's definition, Kimbark [17] proposed that apparent power consists of two orthogonal components, non-active and active power, defined as average power. The non-active power is separated into two components, reactive and distortion power. The first is calculated by equation

$$Q_k = I_{1,\mathrm{RMS}} \cdot V_{1,\mathrm{RMS}} \cdot \sin \varphi_1 \qquad (39)$$

It depends only on fundamental harmonic. The distortion power is defined as non-active power of higher harmonics:

$$D_k = \sqrt{U^2 - P^2 - Q_k^2}. \qquad (40)$$

Sharon's definition

This definition [18], introduces two quantities: reactive apparent power, S_q, and complementary apparent power S_c, defined as:

$$S_q = V_{\mathrm{RMS}} \cdot \sqrt{\sum_{k=1}^{+\infty} I_{k,\mathrm{RMS}}^2 \sin^2 \varphi_k} \qquad (41)$$

and

$$S_c = \sqrt{U^2 - P^2 - S_q^2} \qquad (42)$$

where S is apparent power (9) and P active power(8).

Fryze's definition

Fryze's definition [19] assumes instantaneous current separation into two components named active and reactive currents. Active current is calculated as

$$i_a(t) = \frac{P}{V_{\mathrm{RMS}}^2} v(t) \qquad (43)$$

and reactive current as:

$$i_r(t) = i(t) - i_a(t). \qquad (44)$$

Active and reactive powers are

$$P = V_{\mathrm{RMS}} \cdot I_a$$
$$Q_f = V_{\mathrm{RMS}} \cdot I_r \qquad (45)$$

where I_a and I_r represent RMS values of instantaneous active and reactive currents.

Kusters and Moore's power definitions

Kusters-Moore definition [20] presents two different reactive power parameters, inductive reactive power:

$$Q_{\mathrm{L}} = V_{\mathrm{RMS}} \cdot \frac{\sum_{k=1}^{+\infty} \frac{1}{k} \cdot V_{k,\mathrm{RMS}} \cdot I_{k,\mathrm{RMS}} \cdot \sin \varphi_k}{\sqrt{\sum_{k=1}^{+\infty} \frac{V_{k,\mathrm{RMS}}^2}{k^2}}} \tag{46}$$

and capacitive reactive power:

$$Q_{\mathrm{C}} = V_{\mathrm{RMS}} \cdot \frac{\sum_{k=1}^{+\infty} k \cdot V_{k,\mathrm{RMS}} \cdot I_{k,\mathrm{RMS}} \cdot \sin \varphi_k}{\sqrt{\sum_{k=1}^{+\infty} k^2 \cdot V_{k,\mathrm{RMS}}^2}}. \tag{47}$$

There are other power decompositions, not considered in this paper: Shepard-Zakikhani [21], Depenbrock [22] and Czarnecki decomposition [23, 24]. More comprehensive comparison of reactive power definitions, obtained by means of simulation, can be found in [25].

3. MEASUREMENT SYSTEM

In order to establish a comprehensive picture about the properties of a given load one needs to perform complete analysis of the current and voltage waveforms at its terminals. In that way the basic and the higher harmonics of both the current and the voltage may be found. More frequently, however, indicators related to the power are sought in order to quantitatively characterize the load. Namely, a linear resistive load will have voltage and current in-phase and will consume only real power. Any other load will deviate from this characterization and one wants to know the extent of deviation expressed by as much indicators as necessary to get a complete picture. All these were implemented in our measuring system which will be shortly described in the next.

The solution, as described in full details in [6, 7], is based on a real time system for nonlinear load analysis. The system is based on virtual instrumentation paradigm, keeping main advantage of legacy instruments – determinism in measurement.

The system consists of three subsystems: acquisition subsystem, real time application for parameter calculations, and virtual instrument for additional analysis and data manipulation (Fig. 1).
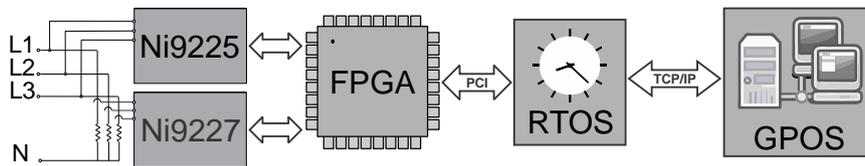
Fig. 1 The system architecture

The acquisition subsystem, Fig. 2, is implemented using field programming gate array (PXI chassis equipped with PXI-7813R FPGA card with Virtex II FPGA) in control of data acquisition [26]. Acquisition is performed using NI 9225[27] and NI 9227 [28] c-series acquisition modules connected to PXI-7813R FPGA card [26]. A/D resolution is

24-bit, with 50 kSa/s sampling rate and dynamic range ±300 V for voltages and ±5 A for currents. The FPGA provides timing, triggering control, and channel synchronization maintaining high-speed, hardware reliability, and strict determinism.

The FPGA code is implemented in a LabVIEW development environment. The function of the FPGA circuit is acquisition control.
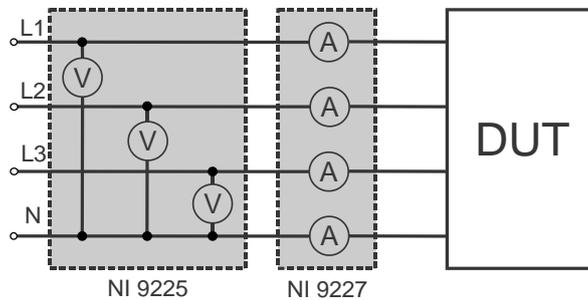
Fig. 2 Connection diagram of acquisition subsystem

The software component is implemented in two stages, executing on real-time operating system (PharLap RTOS, [29, 30]) and general purpose operating system (GPOS). Described system enables calculation of a number of parameters in real-time that characterize nonlinear loads, which is impossible using classical instruments. The measured quantities are calculated from the current and voltage waveforms according to IEEE 1459-2000 and IEEE 1459-2010 standards [12, 13].

Real time application (Fig. 3) calculates power and power quality parameters deterministically and saves calculated values on local storage. The application is executed on real time operating system.
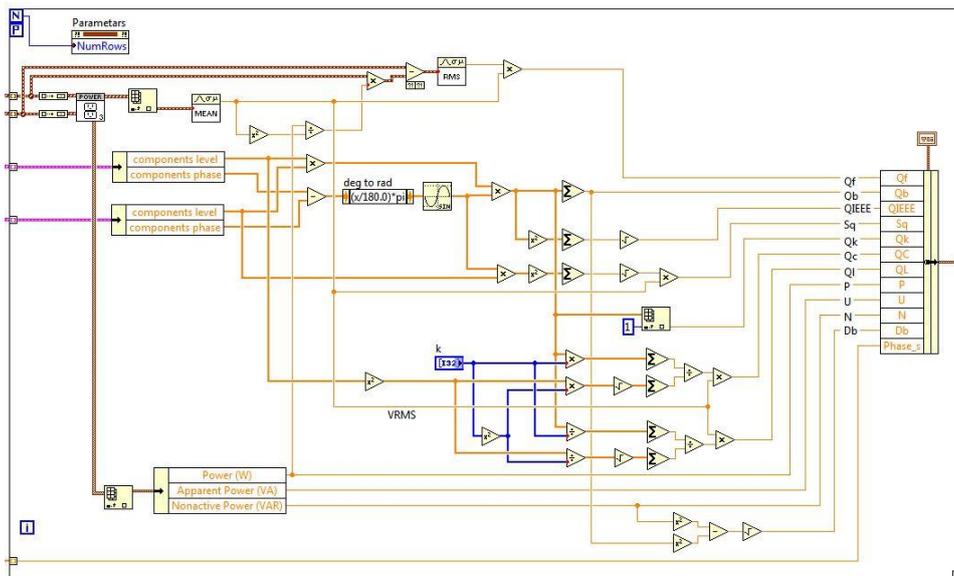
Fig. 3 Part of real-time application in G code, alternative reactive power calculations

Virtual instrument, implemented in National Instruments LabVIEW [30, 31] environment, is used for additional analysis and data manipulation represents user interface of described system. It runs on general purpose operating system, physically apart from the rest of the system. Communication is achieved by TCP/IP. Parameters and values obtained by means of acquisition and calculations are presented numerically and graphically (Fig. 4).
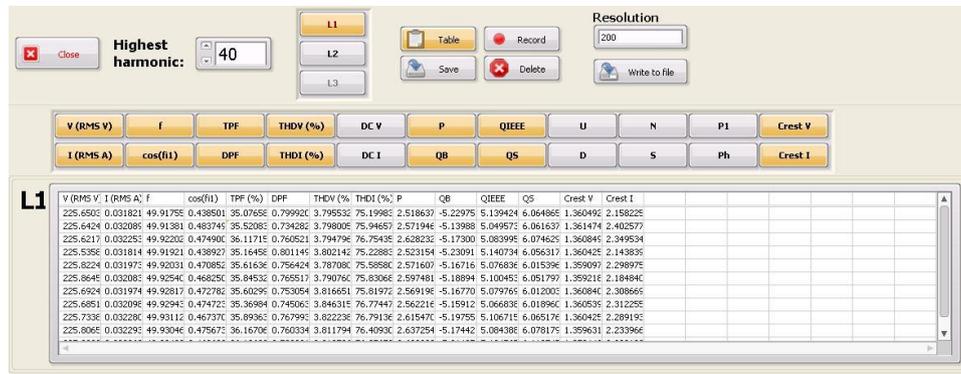
Fig. 4 Virtual instrument provides measurements of various parameters

4. MEASUREMENT RESULTS

We have performed measurements on various small loads. The parameters obtained may be used for decision making of various kinds, such as verification of compliance to some standards or categorization within quality frames. As small loads here we consider various devices: CFL and LED lamps, power supply devices and battery chargers in case of personal communication and computing devices. These devices are ubiquitous and in everyday use, thus their cumulative effect on power distribution grid is not negligible [32], [33]. Various parameters that characterize nonlinearity, efficiency and quality are measured and calculated.

Table 1 shows measured results obtained on small loads such as various compact fluorescent lamps (CFL, 7 W – 20W), incandescent lamps (100W and 60W), two low-power 1 W indoor LED (light emitting diode) lamps, prototype of street 34 W LED lamp and CRT computer monitor for reference.

Compact fluorescent lamp is good example of nonlinear load [34]. It brings reduction in total energy consumption (about 20%, comparing to incandescent lamp of equivalent luminosity), but with harmonic currents and increased harmonic loss on distribution transformer. Measurements show that CFL lamps have good correction of displacement power factor, but significant distortion leading to low total power factor (Table 1). CFLs are equipped by power supply units which conduct current only during a very small part of fundamental period, so the current drawn from the grid has the shape of a short impulse.

Table 1 CFL and LED lamps

Type	Nominal power (W)	Frequency (Hz)	V_{RMS}(V)	I_{RMS} (mA)	Active power (W)	I_{DC} (mA)	Voltage THD(%)	Current THD(%)	Current CREST	Voltage CREST	DPF (%)	$\cos(\varphi)$	TPF (%)
Incandescent	100	50.03	230.20	421.66	97.02	0.62	3.11	3.05	1.52	1.47	99.95	1.00	99.95
CFL bulb	20	50.03	231.49	134.87	18.64	0.24	2.58	112.17	3.38	1.41	66.55	0.90	59.70
CFL tube	20	49.95	231.20	145.89	19.66	0.25	2.84	114.01	4.33	1.44	65.94	0.88	58.28
CFL bulb	15	49.99	231.47	92.16	12.60	0.13	2.82	115.52	3.52	1.41	65.45	0.90	59.08
Incandescent	60	49.97	231.15	257.88	59.58	0.42	2.87	2.84	1.57	1.41	99.96	1.00	99.96
CFL spot	7	49.97	232.48	50.86	7.23	0.19	2.81	104.24	3.24	1.40	69.23	0.88	61.20
CFL bulb	7	50.06	230.95	52.46	7.21	0.28	2.83	112.26	3.42	1.40	66.51	0.90	59.54
CFL bulb	9	50.01	233.20	60.54	8.25	0.11	2.87	116.93	3.60	1.39	64.99	0.90	58.44
CFL tube	11	50.01	233.17	84.34	11.66	0.16	2.79	112.27	3.37	1.45	66.51	0.89	59.28
CFL tube	18	50.01	221.32	135.56	18.40	0.38	2.82	107.35	4.52	1.45	68.16	0.90	61.32
CFL tube	11	50.01	221.14	115.00	14.06	0.16	3.01	119.30	4.06	1.46	64.24	0.86	55.41
CFL helix	11	50.00	221.83	76.73	10.23	0.25	2.96	109.26	4.90	1.47	67.51	0.89	60.09
CFL bulb	9	49.99	232.52	70.06	9.70	0.19	2.84	110.87	3.52	1.43	66.98	0.89	59.53
CFL helix	18	50.01	221.46	138.68	19.01	0.35	2.89	105.56	3.94	1.43	68.77	0.90	61.71
CFL helix	20	50.03	231.19	156.43	21.02	0.20	2.79	111.36	3.91	1.44	66.82	0.87	58.13
CFL tube	15	50.01	221.00	105.09	13.96	0.29	3.16	112.13	4.46	1.40	66.56	0.90	60.11
LED white	1	50.00	217.24	14.96	0.35	0.09	2.36	21.14	1.72	1.38	97.84	0.11	10.79
LED cold w.	1	49.94	217.33	14.95	0.35	0.08	2.36	21.14	1.72	1.38	97.84	0.11	10.79
LED street	34	49.99	216.63	246.12	32.87	0.05	2.53	102.98	3.28	1.38	69.66	0.89	61.66
CRT	–	50.03	232.63	475.86	107.46	1.60	2.93	13.24	1.65	1.49	99.14	0.98	97.69

Characterization of nonlinear loads can be accomplished by analyzing reactive and distortion power. Table 2 shows reactive power and distortion power values, calculated using alternative definitions, for compact fluorescent lamps, two incandescent lamps and indoor LED lamps. Following values are displayed: active power (P), apparent power (S), non-active power (N), Budeanu's reactive power (Q_B), Budeanu's distortion power (D_B), Fryze's reactive power (Q_f), IEEE Std 1459-2010 proposed definition for reactive power (Q_{IEEE}), Shanon's apparent power (S_q), Kimbark's reactive power (Q_k), Kusters-Moore's capacitive (Q_C) and inductive (Q_L) reactive power.

Comparison of Budeanu's reactive and distortion power suggests that all examined CFL and LED lamps are non-linear loads ($D_B>Q_B$). Reactive power calculated from Fryze's definition (45) is equal to non-active power, $N = \sqrt{S^2 - P^2}$. Kimbark's equation (39) for reactive power, which takes only fundamental harmonic into account, gives approximately ±3% deviance from Budeanu's formula (Q_B). It suggests that the actual contribution of harmonic frequencies to reactive power is small – less than 3% of the total reactive power.

IEEE proposed definition always provides value of the total reactive power greater than the value of the fundamental component.

Table 2 CFL and LED lamps

No.	Type	Power	P (W)	U (VA)	N (VAR)	Q_B(VAR)	D_B(VAR)	Q_f (VAR)	Q_{BEEE} (VAR)	S_q (VAR)	Q_k (VAR)	Q_c (VAR)	Q_L (VAR)
1	CFL Rod		11.56	17.84	13.58	-6.16	12.10	13.58	6.16	10.24	-6.16	-4.43	-6.11
2	CFL bulb E27	20	17.14	27.72	21.78	-8.43	20.08	21.78	8.43	14.48	-8.43	-6.46	-8.37
3	CFL tube E27	20	16.77	28.46	23.00	-8.44	21.39	23.00	8.45	14.55	-8.45	-6.07	-8.39
4	CFL bulb E27	15	11.59	18.91	14.94	-5.31	13.97	14.94	5.32	9.22	-5.32	-4.00	-5.28
5	Inc E27	100	86.77	86.78	0.80	-0.50	0.63	0.80	0.50	0.56	-0.50	-0.36	-0.49
6	CFL spot E14	7	5.87	9.32	7.25	-2.83	6.67	7.25	2.81	4.23	-2.81	-2.17	-2.80
7	CFL bulb E27	7	6.16	9.86	7.71	-2.64	7.24	7.71	2.65	4.83	-2.65	-2.03	-2.63
8	CFL bulb E14	9	6.46	10.78	8.63	-2.72	8.19	8.63	2.72	5.45	-2.72	-2.08	-2.70
9	CFL tube E14	11	9.89	16.11	12.72	-4.71	11.82	12.72	4.69	7.89	-4.69	-3.61	-4.66
10	CFL tube E27	18	17.10	28.86	23.24	-8.73	21.54	23.24	8.75	13.27	-8.75	-6.64	-8.68
11	CFL tube E27	11	10.63	17.67	14.12	-5.83	12.85	14.12	5.83	8.85	-5.83	-4.41	-5.79
12	CFL helix E27	11	9.58	16.27	13.16	-4.93	12.20	13.16	4.95	8.75	-4.95	-3.68	-4.90
13	Inc E14	60	55.06	55.06	0.61	-0.37	0.49	0.61	0.37	0.37	-0.37	-0.27	-0.37
14	CFL helix E27	18	17.21	28.87	23.18	-8.82	21.43	23.18	8.83	15.55	-8.82	-6.77	-8.76
15	CFL helix E27	20	18.41	30.68	24.54	-9.95	22.43	24.54	9.93	16.14	-9.93	-7.56	-9.86
16	CFL tube E27	15	12.66	21.97	17.95	-6.32	16.80	17.95	6.33	11.63	-6.33	-4.80	-6.28
17	Spot E27	15	16.92	34.24	29.77	-3.88	29.52	29.77	4.14	20.01	-4.13	-1.98	-4.06
18	Spot E27	10	13.23	26.33	22.76	-2.97	22.56	22.76	3.17	15.45	-3.17	-1.51	-3.12
19	Bulb W E27	8	10.00	19.53	16.77	-2.81	16.54	16.77	2.94	11.52	-2.93	-1.74	-2.89
20	Bulb W E27	6	8.51	9.45	4.11	0.08	4.11	4.11	0.07	3.29	0.07	0.08	0.07
21	Bulb E27	6	8.69	9.58	4.04	0.09	4.04	4.04	0.08	3.28	0.08	0.08	0.08
22	Bulb E27	3	4.07	7.70	6.54	-0.84	6.48	6.54	0.90	4.35	-0.90	-0.45	-0.88
23	RGB E27	3	1.92	3.17	2.52	0.01	2.52	2.52	0.01	1.39	0.00	0.05	0.00
24	Spot E14	3	4.00	8.05	6.99	-0.98	6.92	6.99	1.04	4.86	-1.04	-0.52	-1.02

Further, personal devices such as tablet computer, mobile phone, laptop computer and cordless telephone containing rechargeable batteries are analyzed regarding operating conditions. Measured results are presented in Table 3. Working conditions are standby (device turned off and battery not charging), working and charging (device turned on and battery charging) and charging only (device turned off and battery charging). A standalone battery charger is also tested.

Following values are measured and shown in the table: voltage RMS (V), current RMS (I), frequency (f), cosine of 1st harmonic phase difference ($\cos\varphi_1$), TPF – total power factor (%), DPF – distortion power factor (%), THD$_V$ – voltage total harmonic distortion (%), THD$_I$ – current total harmonic distortion (%), active power (P), Budeanu's reactive power (Q_B), apparent power (U), distortion power (D), non-active power (N), phasor power (S), first harmonic active power (P_1) and higher harmonics active power (P_H).

In the next we will pay some attention to the very results depicted in Table 3. Let's first have a glimpse at the distortions of the current (THD_I). As can be seen even in the best cases the THD_I is larger than 20%. There is a case, a mobile phone battery charger while charging, where the THD_I is 154.51% which means the harmonics exceed by a large margin the fundamental. Note that this is not an isolated case. One may observe several THD_Is of similar value. To summarize, THD_I is exposing the nonlinear character of all small loads, some of which are extremely nonlinear producing harmonics larger than the fundamental one.

Table 3 Personal devices in different working conditions

No.	Device description	V (V)	I (mA)	f (Hz)
1	Charger 230V 1.7A - 2XAAA NiCd battery charging. 850mAh	236.06	9.89	50.02
2	Tablet computer turned on. Li-Polimer 8220 mAh battery charging	235.70	80.92	49.98
3	Tablet computer turned off. Li-Polimer 8220 mAh battery charging	236.59	61.65	49.99
4	Tablet computer turned off. charger 230V/2A connected. not charging	236.51	1.70	50.00
5	Mobile phone charger connected. not charging 230V/0.2A	236.62	1.33	9.99
6	Mobile phone turned on. Li-Ion 1230 mAh battery charging	235.65	53.72	49.98
7	Mobile phone turned off. Li-Ion 1230 mAh battery charging	236.09	48.05	50.01
8	Laptop comp. (type 1) turned on. charger 230V. 1.7A connected, not charging	233.49	22.99	50.01
9	Laptop comp. (type 1) turned on. Li-ION 2200mAh battery charging	232.81	231.39	50.00
10	Laptop comp. (type 1) turned off. Li-ION 2200mAh battery charging	233.52	106.52	49.99
11	Laptop comp. (type 2) turned on. Charger 230V 1.5A connected, not charging	233.07	15.71	49.99
12	Laptop computer (type 2) turned on. Li-ION 4400mAh battery charging	232.05	436.60	49.97
13	Cordless telephone base charger 230V/40mA disconnected	232.77	21.05	49.97
14	Cordless telephone base. 2XAAA. NiCd. 550mAh battery not charging	233.68	21.71	50.00
15	Cordless telephone base. 2XAAA. NiCd. 550mAh battery charging	233.55	25.60	49.99

No.	TPF (%)	DPF (%)	THD_V (%)	THD_I (%)	P (W)	Q_B (VAR)	U (VA)	D (VAR)	N (VAR)	S (VAR)	P_I (W)	P_H(W)
1	32.93	70.81	1.70	94.47	0.77	1.77	2.33	1.62	2.20	1.68	0.78	-0.02
2	57.36	58.15	1.73	137.76	10.94	-1.74	19.07	15.53	15.62	11.08	11.08	-0.14
3	55.12	55.54	1.70	146.23	8.04	-0.93	14.59	12.13	12.17	8.09	8.17	-0.12
4	21.43	79.20	1.67	114.80	0.09	0.18	0.40	0.35	0.39	0.20	0.05	0.00
5	12.64	101.35	1.69	59.01	0.04	0.17	0.31	0.26	0.31	0.18	0.02	0.00
6	52.73	53.66	1.71	154.51	6.67	-1.18	12.66	10.69	10.76	6.78	6.73	-0.05
7	51.18	51.98	1.77	161.72	5.81	-0.96	11.34	9.70	9.75	5.88	5.87	-0.06
8	7.00	95.18	1.78	29.07	0.38	1.38	5.37	1.61	5.36	5.12	0.38	-0.01
9	53.67	54.76	2.00	147.11	28.91	-6.10	53.87	45.04	45.45	29.55	29.65	-0.71
10	47.51	50.62	1.92	164.35	11.82	-4.64	24.87	21.39	21.89	12.70	12.18	-0.28
11	12.69	99.22	1.94	40.82	0.46	1.46	3.66	1.42	3.63	3.37	0.43	0.00
12	96.74	97.30	1.83	20.90	98.01	-10.67	101.31	23.32	25.65	98.59	97.86	0.02
13	23.50	90.76	1.80	43.70	1.15	4.33	4.90	1.97	4.76	4.48	1.16	-0.01
14	47.31	92.64	1.78	36.64	2.40	4.09	5.07	1.81	4.47	4.74	2.43	-0.01
15	70.29	92.99	1.82	37.24	4.20	3.66	5.98	2.16	4.25	5.57	4.23	-0.02

The next very important and also interesting set of data is related to the power factor. In early days it was known as $\cos\varphi$ of the load while only linear loads were considered supposedly having reactive component introducing phase shift between the voltage and the current. The total power factor (TPF) encompasses the whole event including the distortions of both the voltage and the current and their mutual phase shift. As can be seen from Table 1, there is only one case where the TPF is approaching unity which is supposed to be its ideal value. In many of the cases the value of TPF is smaller than 50% meaning that the active power is smaller than a half of the total power drawn from the main which, as we could see from the previous paragraph, is mainly due to the distortions. In general, since most of the chargers are considered of small power (look to the column P1 in Table 3), no power factor correction is built in so that significant losses are allowed. That, to repeat once more, would not be a problem if the number of such devices, being attached to the mains all the time, is not in the range of billion(s).

The next column, the distortion power factor (DPF), represents the percentage of power taken by the harmonics. As we can see, except for a small number of cases where the harmonics are approximately on the level of half of the total power, in most cases they are taking as large power as the fundamental. Note, the harmonics are unwanted not only because of efficiency problems. In fact, in the long term, the presence of harmonics on the grid can cause:

- Increased electrical consumption
- Added wear and tear on motors and other equipment
- Greater maintenance costs
- Upstream and downstream power-quality problems,
- Utility penalties for causing problems on the power grid
- Overheating in transformers, and similar.

Similar conclusion may be drawn in by comparison of the Distortion (D) and the power of the first (fundamental) harmonic (P_1). There are only three cases where the second is larger than the former.

To summarize the data from Table 3 one may say that an electronic load to the grid which in fact represents a power supply of a telecommunication or IT device, represents a small but highly nonlinear load. In many cases the TPF of such a load is in favor of everything but not the active power to be delivered to the device.

5. Conclusion

Due to the changes in the nature of the electrical loads to the grid new aspects of the characterization of the loads to the electrical grid are emerging. These are related mainly to the nonlinearities of modern electronic loads and to the subsystems used for conversion from DC to AC and vice versa that is becoming unavoidable in modern production and distribution systems.

To qualify and quantify the properties of the modern power electrical systems new tools are to be developed being able to cope with the new properties of the signals arising at the grid-to-load and grid to power-producing-facility interface. That stands for both theoretical algorithms for computation and for the very measurement equipment.

In these proceedings we represent our results in development and implementation of a measurement system for small loads that are becoming ubiquitous and consequently of big concern for the quality of the delivered electrical energy. We also present the measurement

results for a broad set of electronic loads revealing many secrets hidden behind the prejudice that these loads are small and unimportant.

Our hardware and software solutions may be characterized as advanced, accurate and versatile while at the same time of low price making them very attractive for practical use being it in laboratory or in field conditions.

REFERENCES

[1] L. Freeman, "The Changing Nature of Loads and the Impact on Electric Utilities", Tech Advantage Expo - Electronics Exhibition and Conference 2009, New Orleans, USA, Feb. 2009, www.techadvantage.org/ 2009ConferenceHandouts/2E_Freeman.pdf.
[2] V. Terzija, V. Stanojević, "STLS Algorithm for Power-Quality Indices Estimation", *IEEE Transactions on Power Delivery*, vol. 24, no. 2, pp. 544-552, April 2008.
[3] G. Goertzel, "An Algorithm for the Evaluation of Finite Trigonometric Series", *The American Mathematical Monthly*, no. 1, vol. 65, pp. 34-35, January 1958.
[4] S. Vukosavić, "Detection and Suppression of Parasitic DC Voltages in 400 V AC Grids", *Facta Universitatis, Series: Electronics and Energetics*, vol. 28, no 4, pp. 527-540, December 2015.
[5] L. Korunović, M. Rašić, N. Floranović, V. Aleksić, "Load Modelling at Low Voltage Using Continuous Measurements", *Facta Universitatis, Series: Electronics and Energetics*, vol. 27, no. 3, pp. 455-465, September 2014.
[6] M. Dimitrijević, V. Litovski, "Power Factor and Distortion Measuring for Small Loads Using USB Acquisition Module", *Journal of Circuits, Systems, and Computers*, vol. 20, no. 5, pp. 867-880, August 2011.
[7] M. Dimitrijević, "Electronic System for Polyphase Nonlinear Load Analysis Based on FPGA", PhD thesis, Niš, 2012 (in Serbian).
[8] M. Dimitrijević, and V. Litovski, "Quantitative Analysis of Reactive Power Definitions for Small Non-linear Loads", In Proc. of the 4th Small Systems Simulation Symposium, Niš, Serbia, 2012, pp. 150-154.
[9] M. Dimitrijević, and V. Litovski, "Real-time virtual instrument for polyphase nonlinear loads analysis", In Proc. of the IX Int. Symp. on Industrial Electronics, INDEL 2012, Banja Luka, B&H, November 2012, pp. 136-141.
[10] M. Andrejević Stošović, M. Dimitrijević, and V. Litovski, "Computer Security Vulnerability as Concerns the Electricity Distribution Grid", *Applied Artificial Intelligence*, vol. 28, pp. 323–336, 2014.
[11] M. Dimitrijević, M. Andrejević Stošović, J. Milojković, V. Litovski, "Implementation of Artificial Neural Networks Based AI Concepts to theSmart Grid", *Facta Universitatis, Series: Electronics and Energetics*, vol. 27, no. 3, pp. 411-424, September 2014.
[12] -,"IEEE Trial-Use Standard Definitions for the Measurement of Electric Power Quantities under Sinusoidal, Non-sinusoidal, Balanced, or Unbalanced Conditions", IEEE Power Engineering Society, IEEE Std. 1459-2000, 30. January 2000.
[13] IEEE Power Engineering Society: IEEE Trial-Use Standard Definitions for the Measurement of Electric Power Quantities under Sinusoidal, Nonsinusoidal, Balanced, or Unbalanced Conditions. IEEE Std. 1459-2010, 2. February 2010.
[14] L. S. Czarnecki, "Harmonics and Power Phenomena", Encyclopedia of Electrical and Electronics Engineering, J. Wiley and Sons, 1999.
[15] A. E. Emanuel, "Power Definitions and the Physical Mechanism of Power Flow", J. Wiley and Sons, 2010.
[16] C. I. Budeanu, "Reactive and Fictitious Powers." Rumanian National Institute, no. 2.,1927.
[17] E. W. Kimbark, "Direct Current Transmission" J. Wiley and Sons, 1971.
[18] D. Sharon, "Reactive Power Definition and Power-factor Improvement in Nonlinear Systems." 1973. In Proc. of Ins Vol. Electric Engineers, vol. 120, pp. 704-706.
[19] S. Fryze, et al., "Elektrischen Stromkreisen Mit Nichtsinusoidalformingem Verfauf von Strom und Spannung." *Elektrotechnische Zeitschriji*, no. 53, vol. 25, pp. 596-599, 1932.
[20] N. L. Kusters, W. J. M. Moore, "On the Definition of Reactive Power under Nonsinusoidal Conditions." *IEEE Trans. Power Apparatus Systems*, no. 99, vol. 5, pp. 1845-1854, 1980.
[21] W. Shepard, P. Zakikhani, "Power Factor Correction in Nonsinusoidal Systems by the Use of Capacitance", *Journal of Physics D: Applied Physics*, no. 6, pp. 1850–1861, 1973.
[22] M. W. Depenbrock, E. T. G. Blindleistung, Fachtagung Blindleistung. Aachen, 1979.

[23] L. S. Czarnecki, "Powers in Nonsinusoidal Networks: Their Interpretation, Analysis and Measurement", *IEEE Trans. Instrumental Measurements*, no. 39, vol. 2, pp. 340-345, 1990.

[24] L. S. Czarnecki, "Physical Reasons of Currents RMS Value Increase in Power Systems with Nonsinusoidal Voltage", *IEEE Trans. in Power Delivery*, no. 8, vol. 1, pp. 437-447, 1993.

[25] M. E. Balci, M. H. Hocaoglu, "Quantitative comparison of power decompositions", *Electric Power Systems Research*, no. 78, pp. 318-329, 2008.

[26] -,"NI PXI-7813R R Series Digital RIO with Virtex-II 3M Gate FPGA." National Instruments.

[27] -, "NI 9225 Operating Instructions and Specifications." National Instruments.

[28] -, "NI 9227 Operating Instructions and Specifications", National Instruments.

[29] C. Jarvis, C., K. Kinsella, P. Timpanaro, "Phar Lap ETS™ – An Industrial-Strength RTOS White Paper."

[30] National Instruments: "LabVIEW Real-Time." National Instruments WEB Page. [URL] http://sine.ni.com/ nips/cds/view/p/lang/en/nid/2381.

[31] National Instruments, "LabVIEW System Design Software."

[32] D. Stevanović, P. Petković, "Smarter Power Meters Reduce Economic Losses at Utility Grid", *Facta Universitatis*, *Series: Electronics and Energetics*, vol. 28, no 3, pp. 407-421, September 2015.

[33] S. Puzović, B. M. Koprivica, A. Milovanović, M. Đekić, "Analysis of Measurement Error in Direct and Transformer-Operated Measurement Systems for Electric Energy and Maximum Power Measurement", *Facta Universitatis*, *Series: Electronics and Energetics*, vol. 27, no. 3, pp. 389-398, September 2014.

[34] M. Etezadi-Amoli, T. Sr. Florence, "Power factor and harmonic distortion characteristics of energy efficient lamps", *IEEE Transactions on Power Delivery*, no. 4, pp. 1965–1969, 1989.